

## *Dynamic Behavior of Sand Bed under Oscillating Water Pressure*

Hiroshi NAGŌ\* and Shiro MAENO\*

(Received February 17, 1986)

### SYNOPSIS

Under the attack of storm waves, there are many destructions of coastal structures in the forms of sinking and sliding. These types of destructions will be in close relation to the dynamic behavior of sand bed around the structures. From this point of view, in this paper, we investigate the characteristics of the pore water pressure and effective stresses in the highly saturated sand bed under oscillating water pressure theoretically. The results indicate that the oscillating water pressure induce the notable drop of strength of sand bed around the structure under certain condition.

### 1. INTRODUCTION

Under the oscillating water pressure on the surface of the sand bed the shear strength of the sand bed decrease. This phenomenon is explained as follows. That is, as is shown in Fig. 1, the excess pore water pressure  $h'$  is induced by the oscillating water pressure which propagate into the sand layer accompanied with the damping in amplitude and the phase lag. It is considered that the increase of the excess pore water pressure brings to the decrease of the effective stress.

From the above point of view, the authors have investigated the

---

\* Department of Civil Engineering

fundamental characteristics of the pore water pressures and effective stresses in the sand bed under the oscillating water pressure. In former reserches [1,2], that treat the vertical one- and two-dimensional models, the fundamental behaviors of the pore water pressure and effective stress in the sand bed are clarified theoretically and experimentally in relation to the properties of the oscillating water pressure and of the constituent materials.

In this study, we investigate the dynamic behavior of sand bed around the structure, mainly taking up the effective stresses.

## 2. OUTLINE OF THE THEORETICAL ANALYSIS

### 2.1 Vertical Two-Dimensional Model

The vertical two-dimensional model as is shown in Fig. 2 was chosen as the subject of the analysis. Model is the sand bed around the structure hatched in the figure. The thickness of the sand bed is  $D$ . The depth of the structure in the sand bed is  $d$ . Such structure can be considered as a simplified model of many typical coastal structures. The oscillating water pressure  $\rho g h_s(t)$  acts on the surface of the sand bed in front of the structure.  $h_0$  in Fig. 3 indicates the mean height

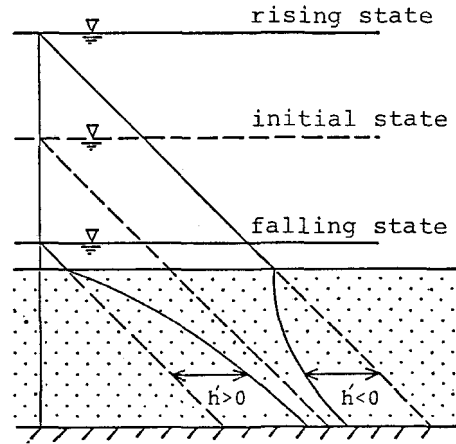


Fig.1 Pore water pressure under oscillating water pressure

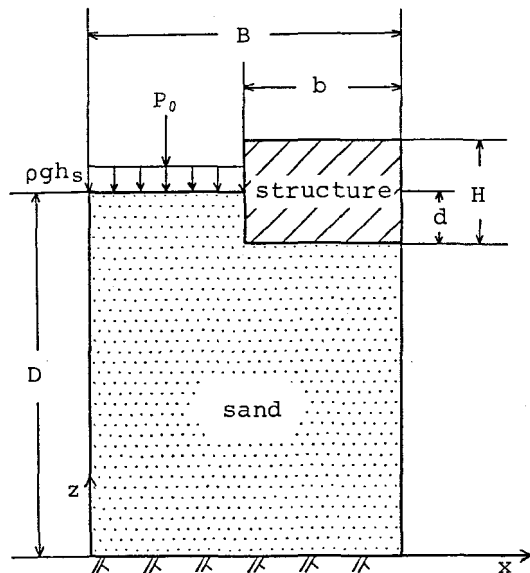


Fig.2 Vertical two-dimensional model

of the oscillating water head  $h_s$  on the sand surface.

The motions of water and sand in the bed are analysed by the same method as for the ground water problems in the elastic sand bed. That is, it is assumed that the skeleton of the sand bed and the water are compressible, and then that the density of the water, the porosity of the sand and the thickness of the sand bed are variable. The void in the bed is occupied by the water and the air. Then, the porosity  $\lambda$  is the sum of the part for the water  $\lambda_w$  and the part for the air  $\lambda_a$ . The pore water moves in accordance with Darcy's law. The volume of the air in the sand bed change in accordance with Boyle's law. Moreover, it is assumed that the boundaries of the sand bed are consist of impermeable boundary except the sand surface.

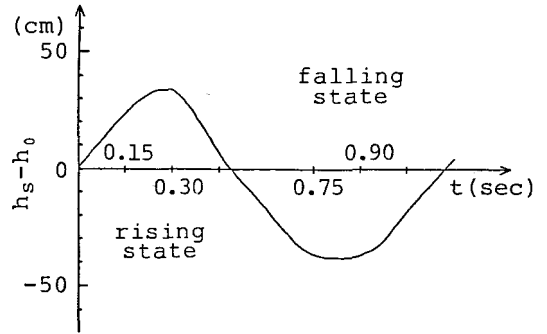


Fig.3 Oscillating water head on the sand surface

porosity  $\lambda$  is the sum of the part for the water  $\lambda_w$  and the part for the air  $\lambda_a$ . The pore water moves in accordance with Darcy's law. The volume of the air in the sand bed change in accordance with Boyle's law. Moreover, it is assumed that the boundaries of the sand bed are consist of impermeable boundary except the sand surface.

## 2.2 Fundamental Equations and Boundary Conditions

For the model mentioned above, the fundamental equations to obtain the distribution of the pore water pressures and displacements of sand are as follows[3,4].

$$\rho g \left( \beta \lambda_w + \frac{\lambda_a}{P_0 + \rho g h} \right) \frac{\partial h}{\partial t} + \frac{\partial}{\partial t} \left( \frac{\partial u_x}{\partial x} + \frac{\partial u_z}{\partial z} \right) = k \left( \frac{\partial^2 h}{\partial x^2} + \frac{\partial^2 h}{\partial z^2} \right) \quad \text{---(1)}$$

$$G \left( \frac{\partial^2 u_x}{\partial x^2} + \frac{\partial^2 u_x}{\partial z^2} \right) + \frac{G}{1-2\nu} \frac{\partial}{\partial x} \left( \frac{\partial u_x}{\partial x} + \frac{\partial u_z}{\partial z} \right) = \rho g \frac{\partial h}{\partial x} \quad \text{---(2)}$$

$$G \left( \frac{\partial^2 u_z}{\partial x^2} + \frac{\partial^2 u_z}{\partial z^2} \right) + \frac{G}{1-2\nu} \frac{\partial}{\partial z} \left( \frac{\partial u_x}{\partial x} + \frac{\partial u_z}{\partial z} \right) = \rho g \frac{\partial h}{\partial z} \quad \text{---(3)}$$

- where,  $\beta$  : compressibility of the water,  
 $\rho$  : density of the water,  
 $g$  : acceleration due to gravity,  
 $P_0$  : atmospheric pressure,  
 $h$  : pore water pressure in head,  
 $u_x, u_z$  : displacement in x- and z- direction respectively,

- $k$  : permeability coefficient,  
 $G$  : shear modulus,  
 $\nu$  : Poisson's ratio,

Fundamental equations are analysed under the following boundary conditions.

- 1)  $h = h_s(t)$  at  $(0 \leq x \leq B-b, z=D)$
- 2)  $\partial h / \partial z = 0$  at  $(0 \leq x \leq B, z=0)$  and  $(B-b \leq x \leq B, z=D-d)$   
 $u_z = 0$  at  $(0 \leq x \leq B, z=0)$
- 3)  $\partial h / \partial x = 0$  at  $(x=0, 0 \leq z \leq D)$ ,  $(x=B, 0 \leq z \leq D-d)$  and  $(x=B-b, D-d \leq z \leq D)$   
 $u_x = 0$  at  $(x=0, 0 \leq z \leq D)$ ,  $(x=B, 0 \leq z \leq D-d)$

### 2.3 Method and Conditions of Calculation

Numerical calculation was carried out by using the Galerkin's finite element method which is one of the weighted residual method. The displacements  $u_x$ ,  $u_z$  and the pore water pressure  $h$  can be obtained by solving the system of fundamental Eqs.(1),(2),(3). The normal effective stresses  $\sigma_x$ ,  $\sigma_z$  and the shear stress  $\tau_{zx}$  are calculated by using stress-strain relationships Eqs.(4),(5),(6). From Mohr's stress circle shown in Fig. 4, the principal stresses  $\sigma_1$  and  $\sigma_3$  are calculated by Eqs.(7),(8). To evaluate the dynamic behavior of sand bed, following two methods are adopted in this study. The first is to investigate the distribution of principal stresses. The second is to compare the angle of internal friction of sand  $\phi'$  with the angle  $\phi$  (called stress angle in this paper) of the tangent to the instantaneous Mohr's circle from the point 0. In the first method, the state

$$\sigma_x = 2G \left\{ \frac{\partial u_x}{\partial x} + \frac{\nu}{1-2\nu} \left( \frac{\partial u_x}{\partial x} + \frac{\partial u_z}{\partial z} \right) \right\} \text{---(4)}$$

$$\sigma_z = 2G \left\{ \frac{\partial u_z}{\partial z} + \frac{\nu}{1-2\nu} \left( \frac{\partial u_x}{\partial x} + \frac{\partial u_z}{\partial z} \right) \right\} \text{---(5)}$$

$$\tau_{zx} = G \left( \frac{\partial u_z}{\partial x} + \frac{\partial u_x}{\partial z} \right) \text{---(6)}$$

$$\sigma_1 = \frac{\sigma_x + \sigma_z}{2} + \sqrt{\frac{(\sigma_x - \sigma_z)^2}{4} + \tau_{zx}^2} \text{---(7)}$$

$$\sigma_3 = \frac{\sigma_x + \sigma_z}{2} - \sqrt{\frac{(\sigma_x - \sigma_z)^2}{4} + \tau_{zx}^2} \text{---(8)}$$

$$\sin \phi \geq \sin \phi' \text{ , } (\sin \phi = \frac{\sigma_1 - \sigma_3}{\sigma_1 + \sigma_3}) \text{---(9)}$$

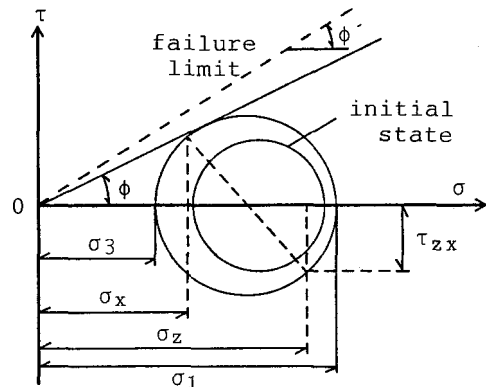


Fig.4 Mohr's stress circle

that the principal stress becomes negative, that is, the occurrence of tensile region is regarded as the failure of sand bed. In the second method, Eq.(4) is applicable for the failure condition. In this paper, the value of  $45^\circ$  is adopted as the value of  $\phi$ . The calculation was carried out under the following conditions.

$$\begin{aligned} D &= 80\text{cm} , B = 60\text{cm} , b = 30\text{cm} , d = 10\text{cm} , H = 20\text{cm} , \\ \lambda_a &= 0.003 , \lambda_w = 0.4 , k = 0.015\text{cm/sec} , \\ \beta &= 43.8 \times 10^{-10} \text{m}^2/\text{kg} (44.6 \times 10^{-11} \text{m}^2/\text{N}) , \\ G &= 3.49 \times 10^7 \text{kg/m}^2 (3.42 \times 10^8 \text{N/m}^2) , \\ \nu &= 0.48 \end{aligned}$$

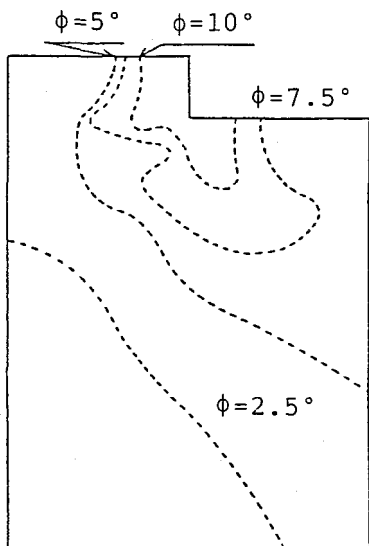
It is assumed that the structure shown in Fig. 2 has its own weight which specific gravity is 2.65. The calculation is started from the initial stress state that obtained by taking account of the weight of the structure.

### 3. RESULTS OF THE ANALYSIS

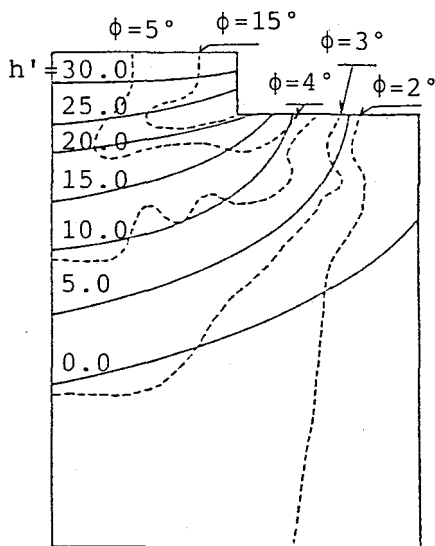
We investigate the dynamic behavior of sand bed on the basis of the results of the analysis on the pore water pressure, stress angle, principal stress and displacement. These physical properties vary with time under the oscillating water pressure. Here, we show, as the representatives, the values obtained for the rising state ( $t=0.30\text{sec}$ ) and falling state ( $t=0.75\text{sec}$ ,  $t=0.90\text{sec}$ ) of the water pressure on the sand surface.

#### 3.1 Pore Water Pressure

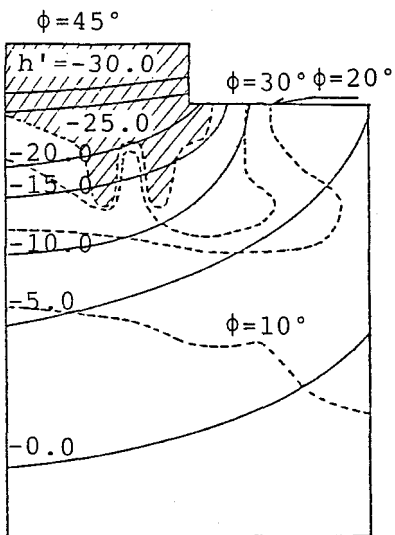
Fig. 5 shows the distribution of excess pore water pressure  $h'$  and stress angle  $\phi$  that are represented by solid line and broken line respectively. This figure shows that the pore water pressure propagates under the structure like the diffraction of wave. The flow characteristics of pore water around the structure are explained as follows. At the rising state, the pore water moves into the under part of the structure. Contrary to this, at the falling state, it moves to the inverse direction. That is, under the oscillating water pressure, the direction of motion of the pore water around the structure varies periodically and the pore water pressure propagates not only to the vertical direction but also to the horizontal direction.



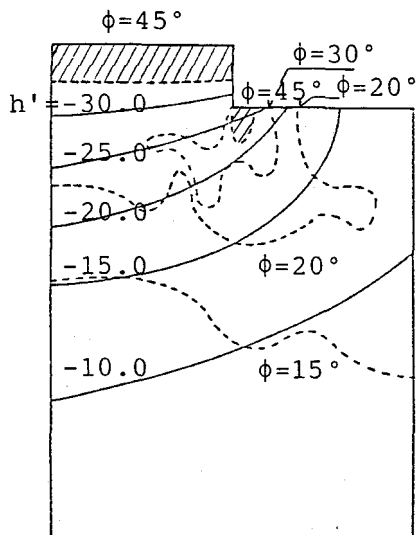
(1) initial state



(2) rising state(t=0.30)



(3) falling state(t=0.75)



(4) falling state(t=0.90)

— : excess pore water head  
 - - - : stress angle

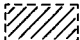
 : failure region

Fig.5 Excess pore water head and stress angle

### 3.2 Stress Angle

In Fig. 5, the hatched zone shows the region which the stress angle  $\phi$  exceeds the internal friction  $\phi' = 45^\circ$ . From this figure, the characteristics of stress angle are explained as follows. At the initial state, the stress angle near the structure is larger than that in the region far from the structure. At the rising state, though the magnitude of the stress angle increases comparing with the initial state, the sand bed is still stable against the failure condition indicated by Eq.(4). But, at the falling state, the failure region appears in front of and under part of the structure. This means that the sand bed around the structure becomes unstable dynamically under such condition.

### 3.3 Principal Stress

Fig. 6 shows the distribution of the principal stresses  $\sigma_1, \sigma_3$  at the initial state, rising state ( $t=0.30\text{sec}$ ) and falling states ( $t=0.75\text{sec}$ ,  $t=0.90\text{sec}$ ). The hatched part shows the tensile region which the minimum principal stress becomes negative. From this figure, the characteristics of the principal stresses are explained as follows. With respect to the plane of the principal stresses, at the initial state, the directions of the maximum principal stresses  $\sigma_1$  under the structure are vertical and almost same as those of  $\sigma_z$ . At the rising state, the plane of the principal stresses changes from the initial state, but at the falling state, it shows the almost same pattern as at the initial state. With respect to the size of the principal stresses, it seems to vary in proportion to the water pressure on the sand surface. Furthermore, the tensile region occurs in the upper layer in front of the structure at the falling state ( $t=0.75\text{sec}$ ). This means that the state of liquefaction which the effective stress becomes to be zero occurs.

### 3.4 Distribution of Displacement

Fig. 7 shows the distribution of the displacement vector at the rising state ( $t=0.15\text{sec}$ ,  $t=0.30\text{sec}$ ) and falling state ( $t=0.75\text{sec}$ ,  $t=0.90\text{sec}$ ). This figure shows the vertical and horizontal movement of sand with the variation of water pressure. At the rising state, the sand right under the structure moves up, and at the falling state,

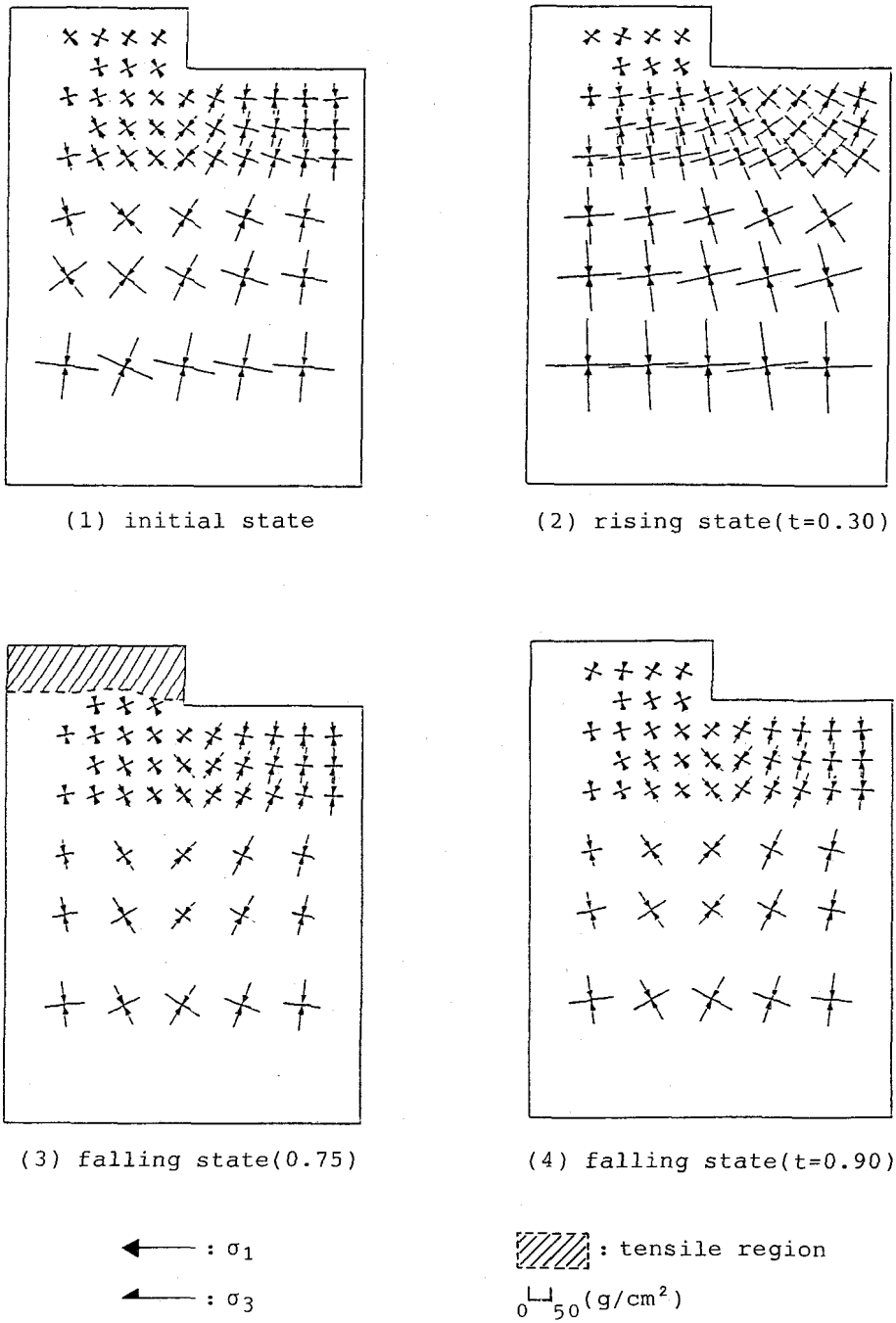


Fig.6 Distribution of principal stress



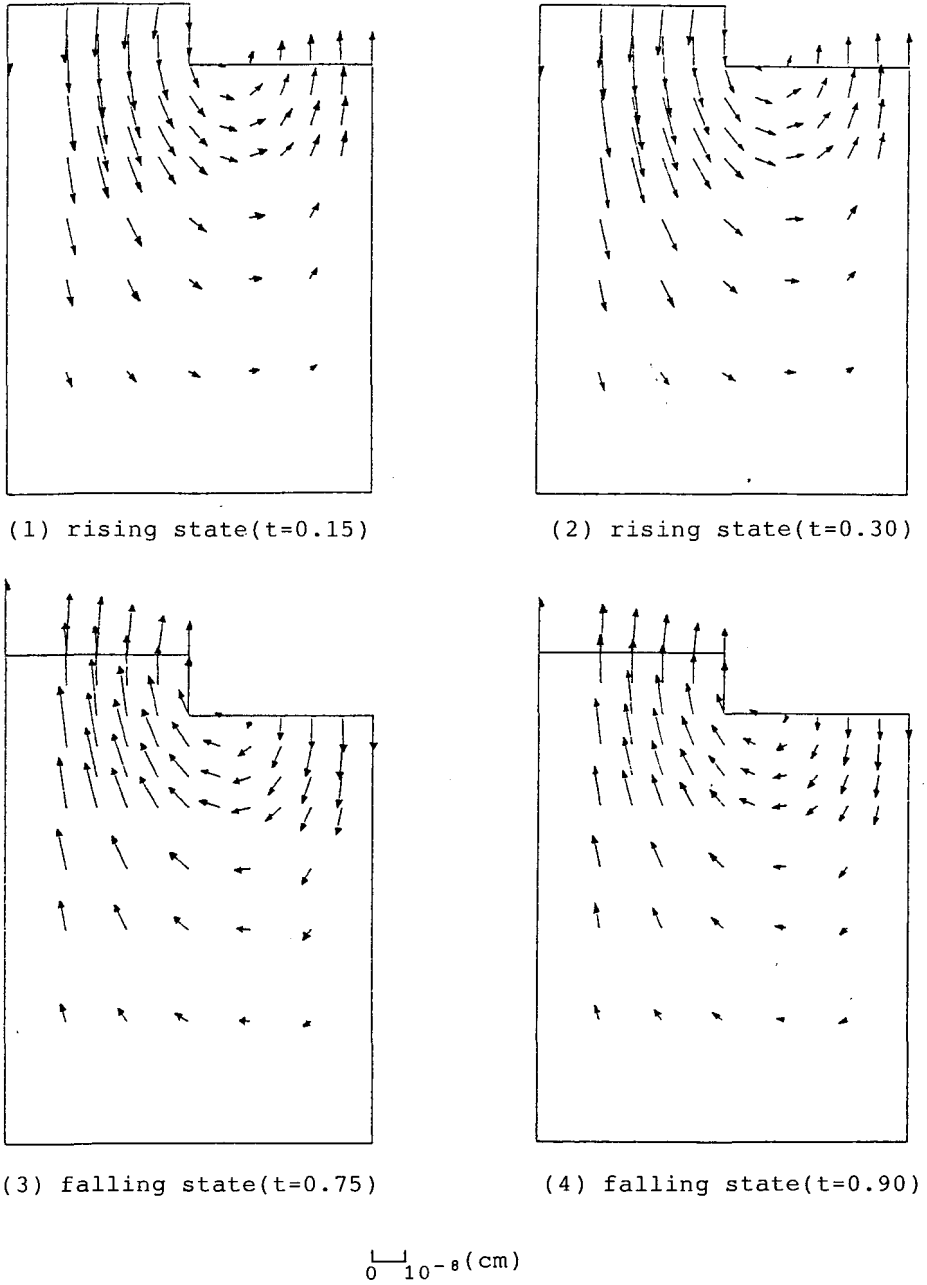


Fig.7 Distribution of displacement

it moves inversely. The horizontal movement is dominant in the under part of the structure. The direction of its movement varies periodically. These features of the displacement agree well with the movement of the pore water.

#### 4. CONCLUDING REMARKS

In this paper the dynamic behavior of sand bed around the structure under oscillating water pressure was analysed theoretically by using the analytical model which has been developed for the highly saturated elastic sand bed.

The dynamic behavior of pore water pressure and sand bed for a given structure-sand bed system was analysed numerically.

The results of analysis shows that the unstable region of sand bed, such as the liquefaction, will occur under a certain condition with the pressure drop on the sand surface. It is considered that the occurrence of such region is in close relation to the dynamical background of several engineering problems, such as sinking of structure, scouring of sand bed in front of the structure, and moving out of sand from the under or inside part of breakwater.

In future studies those will be necessary to estimate quantitatively the dynamic behavior of sand bed in the field, to develop the method to prevent the occurrence of the unstable region in sand bed and to establish the design criteria of the structures under oscillating water pressure.

#### ACKNOWLEDGEMENT

The authors wish to express their gratitude to graduate student, Yasuhiro Nomura, and undergraduate students, Hiroshi Yamada and Shinichi Matsui, for their assistance in computations.

#### REFERENCES

- [1] H. Nagō : Liquefaction of Highly Saturated Sand Layer under Oscillating Water Pressure, Memoirs of the School of Engineering, Okayama Univ., Vol.16, No.1, 1981, pp.91-104.

- [2] H. Nagō and S. Maeno : Pore Water Pressure in sand Bed under Oscillating Water Pressure, *Memoirs of the School of Engineering, Okayama Univ.*, Vol.19, No.1, 1984, pp.13-32
- [3] Biot, M.A. : General Theory of Three-dimensional Consolidation, *J. Appl. Phys.* 12, 1941, pp.155-164.
- [4] De Wiest, R. J. M. : *Flow through Porous Media*, Acad. Press, New York and London, 1969, pp.337-344.